Conditioning data for calculation of the modulation transfer function

Andrew D. A. Maidment and Michael Albert

Conditioning data for calculation of the modulation transfer function

Andrew D. A. Maidment[a] and Michael Albert

Department of Radiology, Thomas Jefferson University, Suite 3390 Gibbon Building, 111 South 11th Street, Philadelphia, Pennsylvania 19107–5563

A method for conditioning data used in the measurement of the modulation transfer function (MTF) is discussed. This method is based upon imposing the constraint that the edge spread function (ESF) is monotonic. The advantages of this technique, when applicable, are demonstrated with simulated examples for which the true MTF is known. The application of this technique in the measurement of the MTF of a digital detector in clinical use is also demonstrated. © *2003 American Association of Physicists in Medicine.* [DOI: 10.1118/1.1534111]

I. INTRODUCTION

The measurement of the modulation transfer function (MTF) is one of the key steps in characterizing a system in terms of linear response theory.[1,2] This measurement can be performed by imaging an object whose spatial frequency content is known, such as a linear object[3] or an edge.[4,5] In the latter case, it is necessary to differentiate[6] the edge spread function (ESF) to obtain the line spread function (LSF). The MTF is then the normalized magnitude of the Fourier transform of the LSF.

While the MTF of most systems is expected to vary smoothly as a function of spatial frequency, noise in the imaging system can result in a measured MTF which fluctuates significantly. Although the noise can generally be reduced by acquiring and averaging over multiple images, this is not always practical or feasible. For example, if MTF measurements are to become part of routine quality assurance for digital detectors (as estimates of the MTF with line-pair phantoms can be problematic[7]) then it is highly desirable that the measurement can be made with a single image acquisition. Attempts to reduce the apparent noise in the MTF without increasing the amount of data acquired have generally taken the form of various regularization procedures, including assuming a Gaussian point spread function,[8] locally fitting to cubic splines,[9] locally fitting to lines,[4] and a variety of smoothing techniques including (in a more general linear systems context) adaptive smoothing.[10,11] All regularization techniques are based upon some *a priori* assumptions about the nature of the detector response. These assumptions have generally fallen into two categories: either an assumed functional form or the assumption that a certain degree of smoothing would not significantly affect the result. In this note we discuss regularization based upon the assumption that the ESF is monotonic. This assumption does not impose an arbitrary functional form on the spread functions and is consistent, for many systems, with expectations based upon the underlying physical principles.

II. BACKGROUND

In measuring the MTF of a digital device using the ESF, an object with a well defined edge is oriented so that the edge is almost parallel to the columns of detector elements and imaged.[3–5] The precise orientation of the edge can be determined from the acquired image. The signal recorded by each detector element is a function of the perpendicular distance of the detector element from the edge. By combining multiple rows of detector elements, the ESF can be super-sampled,[3,4] i.e., sampled with a spacing finer than the spacing between detector elements on the detector surface. Since the MTF is the absolute value of a Fourier transform, the estimation of position of the edge does not affect the final result.

Given a region of interest containing an image of the edge, let x_i be the signed perpendicular distance of the ith detector element from the edge and Y_i the signal in the ith detector element, where the index i assigned to each detector element has been chosen so that $x_i \leq x_{i+1}$. Thus Y_i is an estimate of the ESF at x_i. However, it is often desirable to condition the data, producing a data set $\{y_i\}$ which also serves as an estimate of the ESF but which contains less noise. We propose to obtain such values $\{y_i\}$ by minimizing

$$\chi^2 = \sum_i (y_i - Y_i)^2, \tag{1}$$

subject to the constraints

$$y_i \leq y_{i+1}. \tag{2}$$

This represents a type of quadratic optimization problem which is particularly amenable to solution.[12,13] A detailed solution is described in the Appendix.

In calculating the MTF from the super-sampled data, one must deal with the fact that the combined data from multiple rows does not sample the ESF at uniform intervals. This is due to the fact that the slope of the edge generally is not a simple ratio in terms of the spacing of the detector elements. One method of handling this is to resample the data so as to obtain a uniform sampling interval, for example, by rebinning the data.[3,4] Alternatively, one can calculate the Fourier transform directly from the data. Calculation without resampling has the advantage that one does not need to arbitrarily impose a sampling scheme and one does not introduce any

related artifacts. The chief disadvantage is that, as one can no longer use the fast Fourier transform (FFT) algorithm, the calculation is significantly more time consuming. For instance, without any significant effort at optimization, our calculations without the FFT took a few minutes, compared to on the order of a second for a highly tuned FFT.[14] Several techniques have been recommended for calculating the Fourier transform of nonuniformly spaced data,[15,16] particularly in astronomy where sample times can not be completely controlled, but as the sample spacing here does not vary greatly from uniform spacing we have used a simple direct calculation of the Fourier transform of the derivative:

$$\text{MTF}(f) = C \left| \sum_i W((x_{i+1} + x_i)/2) \right.$$

$$\left. \times (y_{i+1} - y_i) e^{2\pi i f(x_{i+1} + x_i)/2} \right|, \qquad (3)$$

where f is the magnitude of the spatial frequency at which the MTF is being estimated (the direction being perpendicular to the edge), W is an optional windowing function, and the constant C is chosen so that $\text{MTF}(0) = 1$. We have generally used a Hann window,[17]

$$W(x) = 1 - \cos\left(\frac{2\pi(x - x_{\min})}{x_{\max} - x_{\min}}\right), \qquad (4)$$

where $x_{\min}$ and $x_{\max}$ are the limits of the data interval.

III. RESULTS

A. Simulations

Figure 1 shows a numerical example of the application of this technique to an idealized set of data. Figure 1(a) shows the ESF for a one-dimensional detector element which is modeled as being uniformly sensitive along its length and completely insensitive beyond its endpoints. For this example, the length of the detector element is 4 times the sample spacing, and the entire data set consists of 512 samples. Figure 1(b) shows the MTF obtained from the absolute value of the Fourier transform of the derivative of the ESF, normalized to unity at zero spatial frequency. Since the spacing between the detector elements is equal to their lengths, the first two zeros of the MTF in Fig. 1(b) correspond to twice and four times the highest un-aliased frequency supported by the detector array. In Fig. 1(c) additive white noise has been introduced (for the added Gaussian noise, σ corresponds to 1/40 of the difference in the ESF at the endpoints). Figure 1(d) shows the direct calculation of the MTF by taking the Fourier transform of the numerical derivative of Fig. 1(c). Clearly the MTF is significantly degraded by the noise. In Fig. 1(e) the data set from Fig. 1(c) was smoothed with a box-car filter (five sample points wide) before differentiating. The noise in the MTF is reduced, but the value of the MTF is systematically underestimated. In Fig. 1(f) the data from Fig. 1(e) was corrected by dividing by the appropriate sinc function, but this also restores the noise. Figure 1(g) shows the fit to the data from Fig. 1(c) using
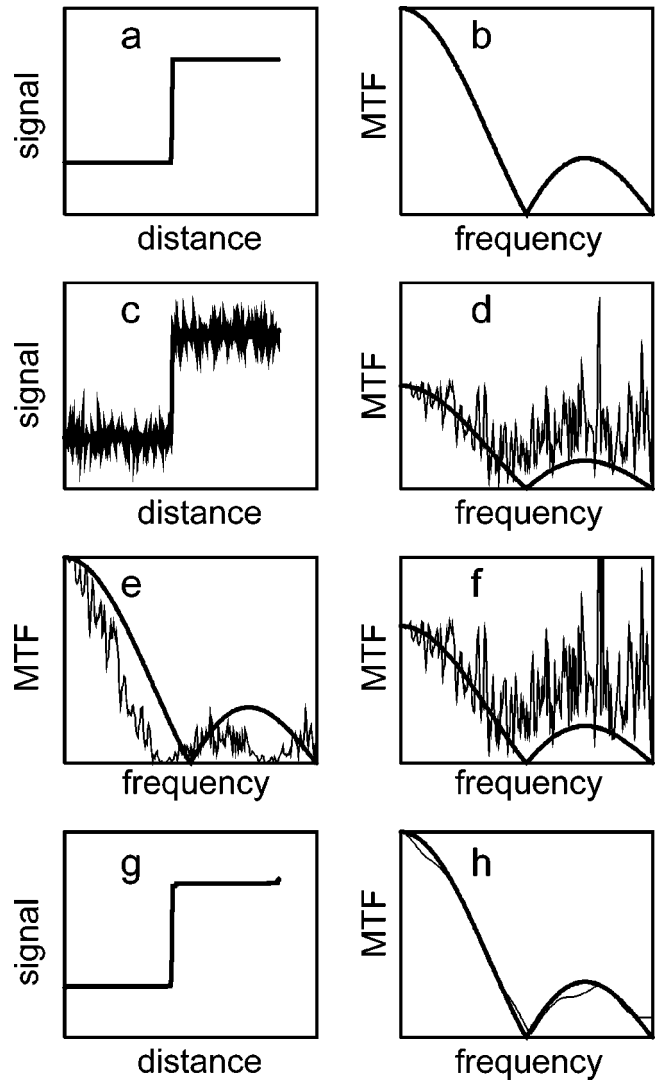

FIG. 1. The ESF (a) of a hypothetical one-dimensional detector element, which integrates uniformly over a region of a given length (here four times the sample spacing), gives an MTF (b) whose shape is the absolute value of a "sinc" function. The addition of noise (c) significantly changes the appearance of the calculated MTF (d). Uncorrected smoothing of the spatial data causes an underestimate of the MTF (e), while correcting the MTF (f) by division by the absolute value of the Fourier transform of the smoothing function gives noise similar to the uncorrected calculation (d). The monotonic fit (g) to the noisy data (c) gives an estimate of the MTF (h) which appears both smooth and without systematic error.

constraints from Eq. (2). Both Figs. 1(g) and 1(h), the resulting estimate of the MTF, show a significant reduction in noise. Further, the estimate of the MTF tracks the known MTF used in the simulation, including the position at which

TABLE I. A comparison of errors in the estimate of the MTF by various metrics for a simple one-dimensional detector. The corresponding graphs are shown in Fig. 1.

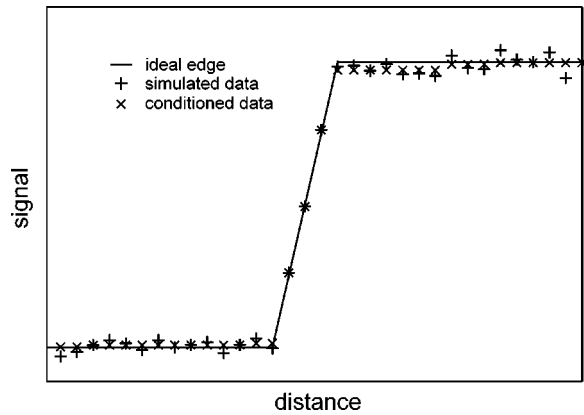| Technique	Max. error	Root-mean-square error	Average error
Direct	1.57	0.419	0.301
Smoothed	0.44	0.199	0.158
Smoothed and corrected	2.22	0.444	0.313
Monotonically constrained	0.06	0.031	0.026

FIG. 2. Details of the simulated one-dimensional detector near the edge, showing the ideal ESF used in the simulation, the simulated data, and the conditioned data.

FIG. 3. Using additive noise with the power spectrum shown in (a), the estimation of the MTF via the ESF was simulated for a detector with 200 μm detector elements. Three different computational procedures are compared: (b) resampling, (c) no resampling, and (d) imposition of the monotonicity constraint and no resampling. In (b), (c), and (d) the dashed curve shows the known MTF used in the simulation.

the MTF vanishes. In Table I the errors in the various techniques of estimating the MTF are compared by means of the maximum, root-mean-square, and average error. In all cases, the estimate based on the monotonicity constraint shows the lowest error, in agreement with visual inspection of the graphs in Fig. 1. Figure 2 shows a superposition of details of Figs. 1(a), 1(c), and 1(g) near the edge. The conditioned fit tracks the simulated data in the region of the edge itself, but away from the edge random fluctuations in the simulated data are quickly dampened by the monotonicity constraint.

Figure 3 shows a more realistic simulated example. The hypothetical detector consists of a two-dimensional array of 200×200 μm elements with 200 μm spacing. The detector response was modeled as a Gaussian transfer function ($\sigma = 20$ μm) convolved with the aperture of the individual detector elements. The aperture was modeled as the convolution of the characteristic functions of two squares with sides 200 μm and 50 μm. Using this model, the image of an edge oriented at 1.7° to the detector grid was simulated. The MTF at this angle is shown as the dark, dashed curve in Figs. 3(b), 3(c), and 3(d). Colored noise with a noise power spectrum (NPS) shown in Fig. 3(a) was introduced additively. The resulting population standard deviation in the values assigned to the individual detector elements was approximately 2% of the change in mean value across the simulated edge. The MTF estimates were then calculated using 50 rows of the simulated array, with 512 detector elements in each row. The angle of the edge relative to the detector array was determined by an automatic fit (as would be necessary in the actual application of the technique). The estimate of the MTF resulting from resampling the ESF data using an algorithm based on rebinning the data points is shown in Fig. 3(b). The result of calculating the MTF without resampling and using a Hann window is shown in Fig. 3(c). The level of noise is similar to the resampled calculation shown in Fig. 3(b). The result of applying the monotonicity constraint of Eq. (2) and calculating the MTF with a Hann window but no resampling [Eq. (3)] give a significant reduction in noise, as shown in Fig. 3(d). Quantitative measures of the error in the estimate of the MTF agree with the visual impression that the mono-
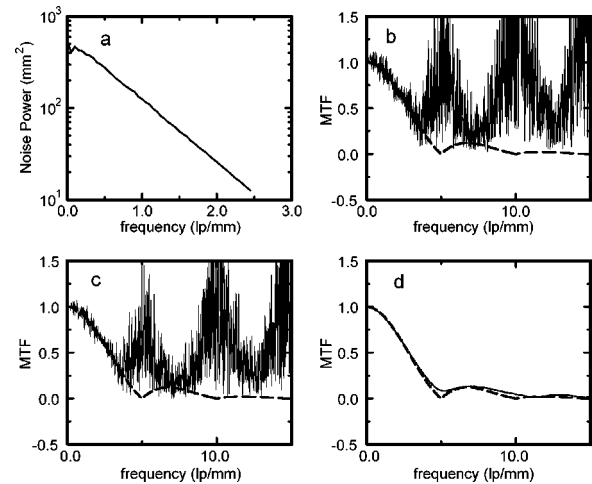
tonic constraint improves the estimate of the MTF, as detailed in Table II. Figure 4 shows a detailed profile near the edge of both the theoretical shape of the ESF used in the simulation, the simulated data, and the conditioned fit. Again, the monotonicity constraint allows the fitted data to follow the simulated data in the region of the edge, but quickly dampens random fluctuations beyond this region. The inset in Fig. 4 illustrates the texture of the colored noise.

B. Practical example

Figure 5 shows the application of this technique to data acquired from a digital detector in clinical use. The MTF test tool consisted of a 27 μm niobium foil with four ground edges arranged in a 5 cm square, supported on a 0.8 mm aluminum sheet 10 cm square. The tool was aligned so that the edges were at a slight angle (measured at 0.86°) to the detector array. The MTF test tool was designed for routine measurement of the MTF.[18] The test tool has now been used in a number of clinical trials of digital mammography. A single image at 28 kVp, 60 mAs was acquired on a prototype of the GE Senographe 2000D full-field digital mammography system. This system incorporates a detector consisting of a large area matrix of photodiodes on an amorphous silicon substrate. The entire detector is coated with a layer of CsI(Tl). The detector element size is approximately 100 μm

TABLE II. A comparison of errors in the estimate of the MTF by various metrics for a two-dimensional detector. The corresponding graphs are shown in Fig. 3.

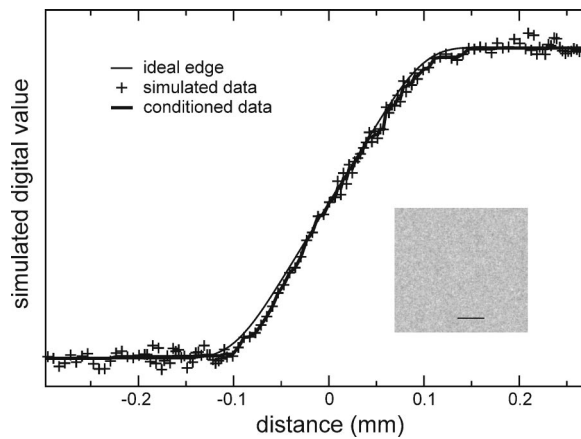| Technique	Max. error	Root-mean-square error	Average error
Resampled	3.75	0.769	0.533
Un-resampled	3.38	0.596	0.400
Monotonically restrained	0.09	0.028	0.022

FIG. 4. Details of the simulated two-dimensional detector near the edge being imaged, showing the ideal ESF used in the simulated, the simulated data, and the conditioned data. The inset demonstrates the appearance of the colored noise used in the simulation (the horizontal bar is 1 cm long).

and digitization is performed to a precision of 14 bits/pixel. The system uses a mammography unit that is essentially identical to the GE DMR mammography system used for screen-film mammography. For clinical image processing, the GE system applies a logarithmic rescaling and a proprietary peripheral equalization algorithm to the images after dark subtraction and flat-fielding. As a prototype, both the raw (dark subtraction and flat-fielding only) and processed (rescaled and peripherally equalized) images were available. The raw images were used in the calculation of the MTF. A region of interest consisting of 60 rows of data each 256 samples long straddling the edge was then selected for analysis. In Fig. 5, curve (A) shows the MTF calculated using resampling, curve (B) show the MTF calculated without resampling, and curve (C) shows the curve calculated using the monotonicity constraint. Again, the monotonicity constraints greatly reduces the noise in the estimated MTF.

IV. DISCUSSION

All methods of measuring the MTF of a system rely upon measuring the spectral response to a known signal. The image of a sharp edge is relatively easy to produce and contains all spatial frequencies (or more precisely, all spatial frequencies whose frequency vector is perpendicular to the edge). By slanting the edge slightly relative to the matrix of detector elements one can obtain a super-sampled data set which allows one to estimate the response of the detector at frequencies above the highest unaliased frequency supported by the detector array. The MTF can then be estimated by calculating the Fourier transform of the derivative of the ESF.

Estimation in this manner tends to introduce a significant amount of noise in the estimate of the MTF. All methods of reducing this noise depend upon *a priori* assumptions about the nature of the MTF. Generally these assumptions result in a smoothing of either the spatial or frequency data. In either case, this can lead to systematic errors in the estimate of the MTF. Smoothing the spatial data tends to underestimate the response at high spatial frequencies, as convolution with the
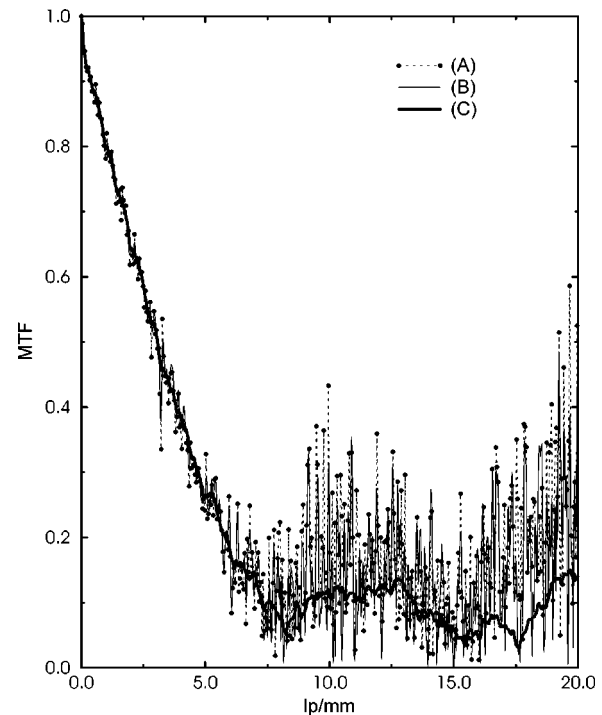

FIG. 5. Demonstration of the estimation of the MTF for a detector in clinical use (GE Senographe 2000D) with 100 μm spacing of detector elements. Curve (A) shows the estimated MTF based upon resampling, curve (B) shows the estimated MTF based on a Fourier transform without resampling, and curve (C) shows the result of the monotonicity constraint and no resampling.

smoothing kernel corresponds to multiplication in frequency space with a function which decreases at high frequencies. Smoothing the MTF can lead to the systematic loss of features such as peaks and valleys in the MTF.

The use of monotonicity of the ESF as a constraint introduces an alternative which, to the best of our knowledge, has not been previously investigated. As seen in the examples, this constraint reduces the noise in the MTF. The two simulated examples indicate that, when applicable, the use of this constraint does not distort the MTF. Further, the application to an actual, clinical system showed no difficulty.

One particular aspect of the use of this constraint is that it is "adaptive" in the sense that near the edge the fitted function is able to change rapidly, while as one moves away from the edge the fit is more and more constrained by the accumulated data points. This is significant because in estimating the MTF by more conventional methods, the length of the rows of data used in the calculation represents a compromise between the desire to measure low-frequency components (which requires long data rows) and the desire to reduce noise in the estimated MTF (by using data rows of moderate length). The nature of this compromise is made clear in light of the fact that the variance in the estimate of each Fourier component is proportional to the row-length, while the expectation value of each Fourier component rapidly approaches its asymptotic limit once the length of the rows is great enough to properly contain the edge. Indeed for most practical digital detectors most of the power in the derivative

of the ESF occurs within a distance from the edge of only a few times the detector spacing. By using monotonicity, data far from the edge is highly constrained, so that the noise in the Fourier components does not increase with increasing row length.

As with other methods for measuring the MTF using the image of a sharp edge, this technique relies on several criteria being satisfied. First, if the edge is not sufficiently sharp then the apparent MTF of the detector will be decreased. Second, if the edge curves appreciably over the region of interest being analyzed, this will also produce an apparent broadening of the LSF and decrease the apparent MTF. Third, as with similar techniques, the region-of-interest must be chosen sufficiently small so that nonuniformity in the x-ray flux does not cause unacceptable systematic errors. While a major advantage of the regularization procedure discussed here is that increasing the size of the region-of-interest (in the direction perpendicular to the edge) does not greatly increase the statistical noise in the estimate of the MTF, this procedure does not aide in distinguishing spatial variations associated with the response function from spatial variations due to nonuniformity of the incident x-ray flux.

The use of the monotonicity constraint may be misleading if the detector shows significant structural nonuniformity. For example, some types of detectors present problems in that the geometric arrangement of the regions to which the detector elements respond is not easily determined with precision, such as detectors using bundles of optical fiber tapers. To the extent that such artifacts are evident, the system violates the assumptions of shift-invariance upon which the definition of the MTF is based. In general, such effects are not so large as to render the MTF useless, although the use of non-Fourier based techniques has been suggested.[19] The data conditioning described in this paper does not address these issues.

As with any *a priori* constraint, monotonicity is only useful when the constraint is (at least approximately) valid. In particular, some detectors show overshoot and undershoot in the ESF, as in xeroradiography. Clearly, this technique would distort the MTF of such devices by removing the overshoot and undershoot. Given these caveats, for appropriate devices the monotonicity constraint should be useful, particularly when the amount of data available is limited, as shown by the examples in this paper.

ACKNOWLEDGMENTS

APPENDIX: MINIMIZATION PROCEDURE

The minimization problem given by Eq. (1) subject to the monotonicity constraint, Eq. (2), is a special case of a class of problems which can be solved by the techniques of quadratic programming. The case is sufficiently special that it is worth discussing the algorithm for its solution without reference to the more general problems handled by quadratic programming.

Slightly generalizing the problem, given data $Y_1, Y_2, \ldots, Y_N$, the goal is to minimize

$$\chi^2 = \sum_i w_i (y_i - Y_i)^2, \tag{A1}$$

subject to the monotonicity constraint

$$y_1 \leq y_2 \leq \cdots \leq y_N, \tag{A2}$$

where the $\{w_i\}$ are positive weights associated with the measured values. In the main text we have treated the weights associated with each of the data points as being equal to a common value, so that this common value can be factored out (or equivalently, set $w_i = 1$). In a more careful treatment one might take each weight as the reciprocal of the variance in the corresponding detector element, but it is questionable as to whether this will greatly improve the precision of the result, and in any case would require the acquisition of multiple data sets, which is a requirement we are attempting to avoid.

Any collection of values $\{y_i\}$ satisfying the monotonicity constraint is said to be *feasible*. Considered as points in $\mathfrak{R}^N$, the set of feasible (i.e., potential) solutions is a convex set (i.e., given two feasible solutions in $\mathfrak{R}^N$, all points on the line segment between them are also feasible). The function χ^2 is itself *strictly convex*, i.e., given two points $\{y_i\}$ and $\{y_i'\}$ in $\mathfrak{R}^N$ the value of χ^2 at any point on the line segment between the two points is less than the value estimated by linear interpolation from the endpoints, with equality only at the endpoints.

Lemma 1: If for some index m, $Y_m > Y_{m+1}$, and $\{y_i\}$ is a feasible solution, then there is a value y' such that when y_m and y_{m+1} in $\{y_i\}$ are both set equal to y', the result is a feasible solution for which the value of χ^2 is not greater than for the original $\{y_i\}$.

Proof: Since $\{y_i\}$ is feasible, $y_m \leq y_{m+1}$. If $y_m \geq Y_{m+1}$, let $y' = y_m$. If $y_m < Y_{m+1}$, let y' be the lesser of the two values Y_{m+1} and y_{m+1}.

Lemma 2: If $Y_m > Y_{m+1}$, then one can reduce the search for a minimum to a search in $\mathfrak{R}^{N-1}$ as follows. Let $\{z_j\}$ be an $N-1$ vector, with constraint $z_1 \leq z_1 \leq \cdots \leq z_{N-1}$, and let

$$\tilde{\chi}^2 = \sum_j \tilde{w}_j (z_j - Z_j)^2, \tag{A3}$$

where

$$Z_i = Y_i, \quad \tilde{w}_i = w_i, \quad i < m,$$

$$Z_m = \frac{w_m Y_m + w_{m+1} Y_{m+1}}{w_m + w_{m+1}}, \quad \tilde{w}_m = w_m + w_{m+1}, \tag{A4}$$

$$Z_i = Y_{i+1}, \quad \tilde{w}_i = w_{i+1}, \quad i > m,$$

and translate the minimization of the new problem back to the original via

$$y_i = z_i, \quad i < m,$$

$$y_m = y_{m+1} = z_m, \tag{A5}$$

$$y_{i+1} = z_i, \quad i > m.$$

Proof: By the first lemma, the search can be confined to the feasible solutions which satisfy the additional constraint $y_m = y_{m+1} = y'$. Translating y' to z_m, the relevant terms of χ^2 can be written as

$$w_m(y' - Y_m)^2 + w_{m+1}(y' - Y_{m+1})^2$$
$$= (w_m + w_{m+1})(z_m - Z_m)^2 + w_m(Y_m - Z_m)^2$$
$$+ w_{m+1}(Y_{m+1} - Z_m)^2, \tag{A6}$$

where Z_m is the weighted average of Y_m and Y_{m+1}. As Y_m, Y_{m+1}, and Z_m are constants, only the first term on the right is relevant in the search for the point $\{y_i\}$ which minimizes χ^2, and relabeling the relevant quantities gives the lemma.

By applying Lemma 2, one can iteratively reduce the dimensionality of the problem until the data itself $\{Z_i\}$ is monotonic, at which point the solution is simply $z_i = Z_i$. This also proves the existence and uniqueness of the solution, as at each reduction of the dimensionality one obtains a statement of the problem equivalent to the previous one, and for the final version of the problem the data itself is monotonic.

[a] Author to whom coprrespondence should be addressed; electronic mail: Andrew.Maidment@mail.tju.edu

[1] C. E. Metz and K. Doi, "Transfer function analysis of radiographic imaging systems," Phys. Med. Biol. **24**, 1079–1106 (1979).

[2] M. Albert and A. D. A. Maidment, "Linear response theory for detectors consisting of discrete arrays," Med. Phys. **27**, 2417–2434 (2000).

[3] H. Fujita, D.-Y. Tsai, T. Itoh, K. Doi, J. Morishita, K. Ueda, and A. Ohtsuka, "A simple method for determining the modulation transfer function in digital radiography," IEEE Trans. Med. Imaging **11**, 34–39 (1992).

[4] P. F. Judy, "The line spread function and modulation transfer function of a computed tomographic scanner," Med. Phys. **3**, 233–236 (1976).

[5] S. E. Reichenbach, S. K. Park, and R. Narayanswamy, "Characterizing digital image acquisition devices," Opt. Eng. **30**, 170–177 (1991).

[6] I. A. Cunningham and A. Fenster, "A method for modulation transfer function determination from edge profiles with correction for finite-element differentiation," Med. Phys. **14**, 533–537 (1987).

[7] M. Albert, D. J. Beideck, P. R. Bakic, and A. D. A. Maidment, "Aliasing effects in digital images of line-pair phantoms," Med. Phys. **29**, 1716–1718 (2002).

[8] E. L. Nickoloff and R. Riley, "A simplified approach for modulation transfer function determinations in computed tomography," Med. Phys. **12**, 437–442 (1985).

[9] K. W. Logan, K. A. Hickey, and S. R. Bull, "Gamma camera MTFs from edge response function measurements," Med. Phys. **10**, 361–364 (1983).

[10] A. Stenman, F. Gustafsson, D. Rivera, L. Ljung, and T. McKelvey, "On adaptive smoothing of empirical transfer function estimates," Control Eng. Pract. **8**, 1309–1315 (2000).

[11] A. Stenman and F. Gustafsson, "Adaptive smoothing methods for frequency-function estimation," Automatica **37**, 675–685 (2001).

[12] D. P. Bersekas, *Nonlinear Programming* (Athena Scientific, Belmont, MA, 1995).

[13] J. N. Franklin, *Methods of Mathematical Economics* (Springer-Verlag, New York, 1980).

[14] M. Frigo and S. G. Johnson, "FFTW: An adaptive architecture for the FFT," in Proceedings of the 1998 IEEE International Conference on Acoustics, Speech and Signal Processing, Piscataway, NJ, 1998, pp. 1381–1384.

[15] N. R. Lomb, "Least-squares frequency analysis of unequally spaced data," Astrophys. Space Sci. **39**, 447–462 (1976).

[16] W. H. Press, S. A. Teukolsky, W. T. Vetterling, and B. P. Flannery, *Numerical Recipes in C* (Cambridge University Press, Cambridge, 1992).

[17] F. J. Harris, "On the use of windows for harmonic analysis with the discrete Fourier transform," Proc. IEEE **66**, 51–83 (1978).

[18] G. Mawdsley, M. Yaffe, A. Maidment, L. Niklason, M. B. Williams, and B. Hemminger, "Acceptance testing and quality control of digital mammography equipment," in *Digital Mammography '98*, edited by N. Karssemeijer, M. Thijssen, J. Hendricks, and L. van Erning (Kluvier, Holland, 1998), pp. 437–444.

[19] H. H. Barrett, J. L. Denny, R. F. Wagner, and K. J. Myers, "Objective assessment of image quality. II. Fisher information, Fourier crosstalk, and figures of merit for task performance," J. Opt. Soc. Am. A **12**, 834–852 (1995).